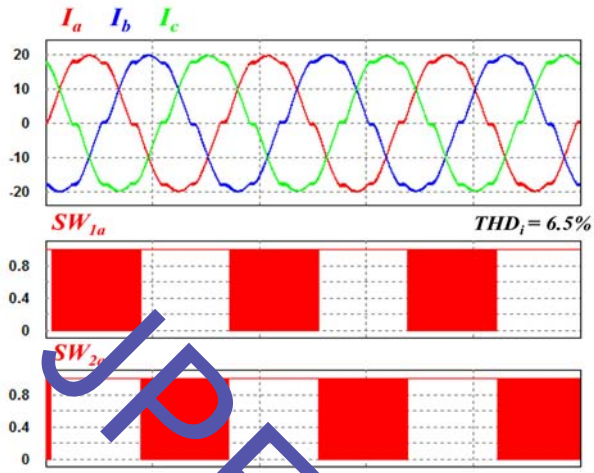

Fig. 16. Simulated currents and switching signals for the conventional CB-PWM.

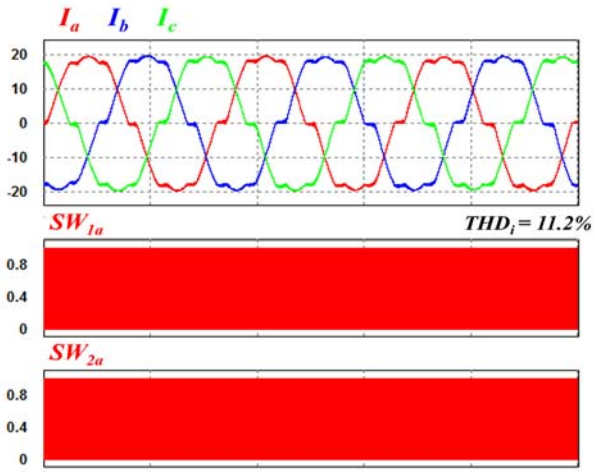

Fig. 17. Simulated currents and switching signals for the synchronous CB-PWM.

TABLE I
SIMULATION PARAMETERS

Parameter	Value
Line-to-line voltage	220 $V_{ll,rms}$
Line frequency	60 Hz
Filter inductance (L_f)	3.5 mH
Filter resistance (R_f)	0.5 Ω
DC-link voltage	450 V
DC-link capacitor	550 uF
Rated power	5 kW
Switching frequency	10 kHz
Control period	100 us

Assuming that θ_Z and θ_{pf} are the same, I_{de} can be calculated as

$$I_{de} = \sqrt{\frac{I_{qe}^2 \theta_Z^2}{1-\theta_Z^2}}. \tag{10}$$

When (10) is used, the optimal reactive current can be injected, thereby reducing the current distortion.

In case the reactive current is injected, when substituting (10) into (7), θ_{pf} can be represented by only θ_Z. θ_{pf} is expressed as

$$\theta_{pf} = \cos^{-1}\left(\sqrt{1-\theta_Z^2}\right). \tag{11}$$

Following (11), the power factor is also represented by θ_Z.

$$\sqrt{1-\theta_Z^2} = \cos\left(\theta_{pf}\right). \tag{12}$$

The power factor depending on θ_Z is shown in Fig. 15, where 0.15 rad/s in the x-axis corresponds to 10°. The power factor decreases as θ_Z increases. θ_Z consistently exists in the Vienna rectifier and is affected by the filter inductance and the grid current. In the experimental condition, the maximum value of θ_Z is approximately 0.12 rad/s at the rated power.

The power factor of the proposed algorithm is slightly lower than that of the conventional CB-BPWM because of the injection of the reactive current. However, the magnitude of the reactive current is small compared with that of the active current. Thus, the Vienna rectifier can control the power factor to near unity. The distortion of the grid current is likewise reduced without a large change in the power factor.

The information of the power factor and the impedance angle must be used to implement the proposed algorithm. Here, we consider the fundamental component. The power factor can be simply approximated by (7) with the active and reactive currents, which are calculated by the sampled grid current. The impedance angle can be also obtained by the filter inductor and the sampled grid voltage and current. When harmonic currents occur because of the distorted grid voltage, an error occurs in the calculated power factor angle and impedance angle. This error can be reduced by using the digital low pass filter on DSP, because the grid voltage and current used in the calculation appear as DC components when only the fundamental components are considered.

IV. SIMULATION RESULTS

Simulations were implemented using a PSIM tool to demonstrate the effectiveness of the synchronous CB-PWM technique with the algorithm for improving current distortion for a Vienna rectifier. The simulation parameters are listed in Table II. The circuit used in the simulation is depicted in Fig. 1.

The simulated grid currents and switching signals of the a-phase when the conventional CB-PWM technique is used

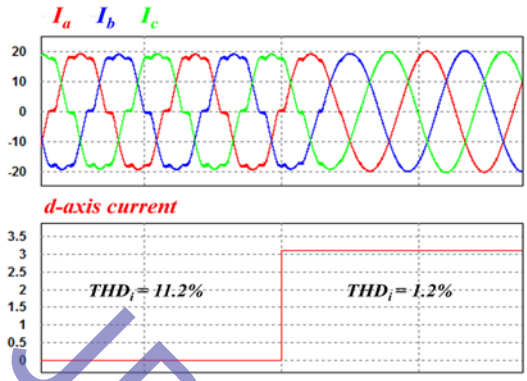

Fig. 18. Results of simulations performed using the proposed algorithm for improving current distortion.

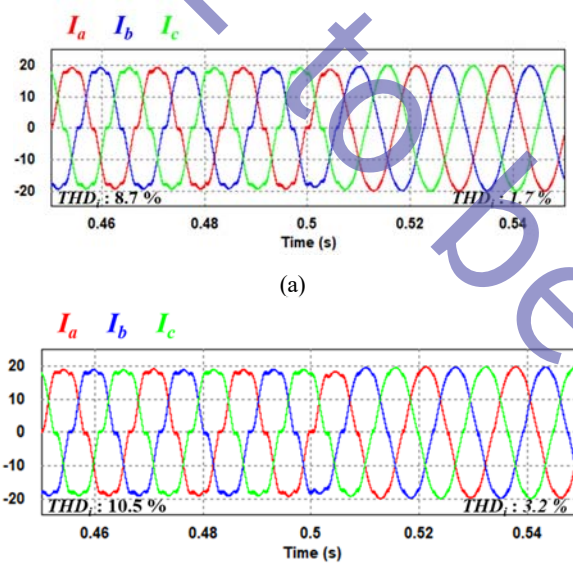

Fig. 19. Performance of the proposed method under distorted voltage. (a) 5th: 3%, 7th: 2%. (b) 5th: 5%, 7th: 3%.

are presented in Fig. 16. The switching signals are asynchronous, and the input currents are distorted near the zero-current point when the relevant requirement is not satisfied, as shown in the figure. THDi is approximately 6.5%.

The simulation results of the synchronous CB-PWM switching method are shown in Fig. 17. The switching signals are synchronous, and SW1 and SW2 are switched simultaneously. In comparison with the results depicted in Fig. 16, the grid currents around the zero crossing are more distorted because of the injection of the unnecessary voltage vectors. THDi increases to 11.2%.

The effectiveness of the proposed algorithm for improving current distortion seen with the synchronous CB-PWM switching method is shown in Fig. 18. The distortion of the grid currents is reduced by injecting the optimal reactive

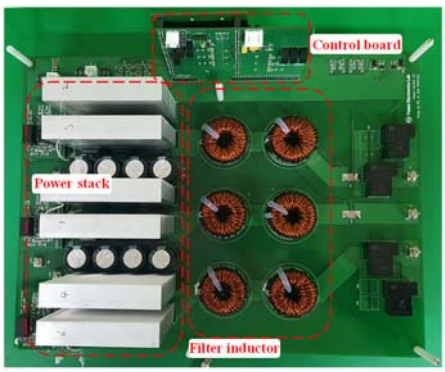

Fig. 20. Prototype of a Vienna rectifier used in the experiments.

current, thereby equalizing the phase of the current and the reference voltage (Fig. 14). In the rated power condition, the q-axis current is 20 A and the d-axis current is 2.5 A. The magnitude of the reactive current is extremely small compared with the active current. Consequently, the power factor is controlled to near unity. In addition, THDi is approximately 1.2%, which is an approximate 10% improvement compared with the results in Fig. 17.

The current distortion under the distorted grid voltage is shown in Fig. 19. The conventional CB-PWM switching method is used before 0.5 s, and the proposed switching method with the optimal reactive is applied after 0.5 s. To simulate the distorted grid, we add the fifth and seventh harmonic voltages, which are injected with a ratio based on the magnitude of the grid voltage, to the simulation condition. Before 0.5 s, THDi is increased compared with that in Fig. 16 because of the distorted voltage. When the proposed method is used, THDi drastically decreases after 0.5 s. However, the current distortion by the distorted voltage remains, though the current distortion by the proposed switching method and impedance angle disappears, as shown in Fig. 19. Therefore, the THDi of Fig. 19 is higher than that of Fig. 18.

V. Experiment Results

This section presents the results of experiments conducted to verify the performance of the proposed synchronous CB-PWM switching method with an optimal reactive current injection to improve current quality. The parameters of the experiment are the same as the simulation parameters listed in Table II.

Experiments were conducted using a set of prototypes of a Vienna rectifier rated at 5 kW (Fig. 20). The prototype consists of a control board, a power board, and filter inductors. A digital signal processor (TMS320F28335 DSP) is used in the control board. The power board comprises the rectifier and the filter inductor. The THD and power factor of the current were measured using a WT3000 power analyzer.

The experimental results at rated power conditions are shown in Fig. 21. Under these conditions, the Vienna rectifier

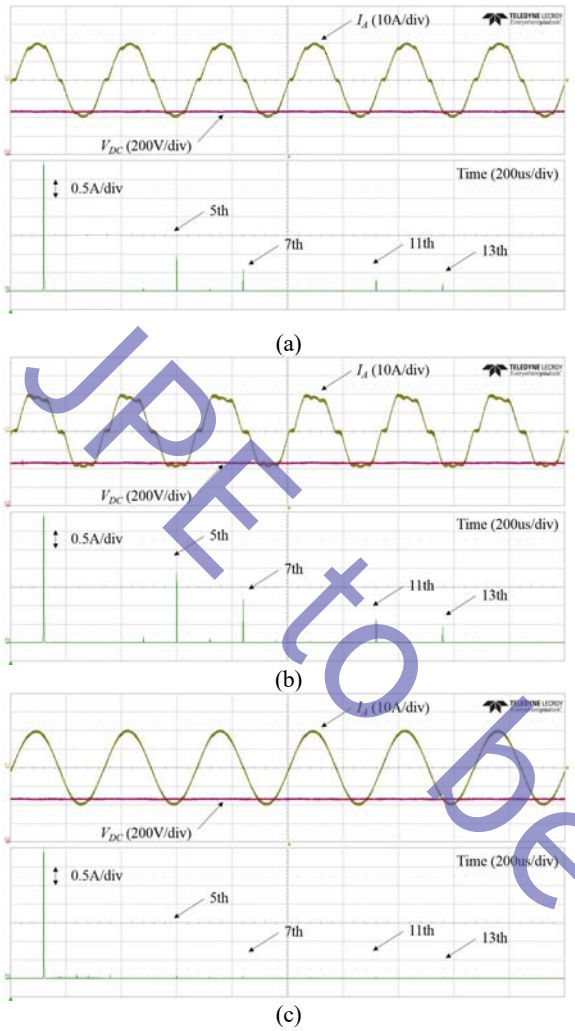

Fig. 21. Experiment results in the rated load condition. (a) Conventional CB-PWM. (b) Proposed synchronous CB-PWM. (c) Proposed synchronous CB-PWM and optimal reactive current injection.

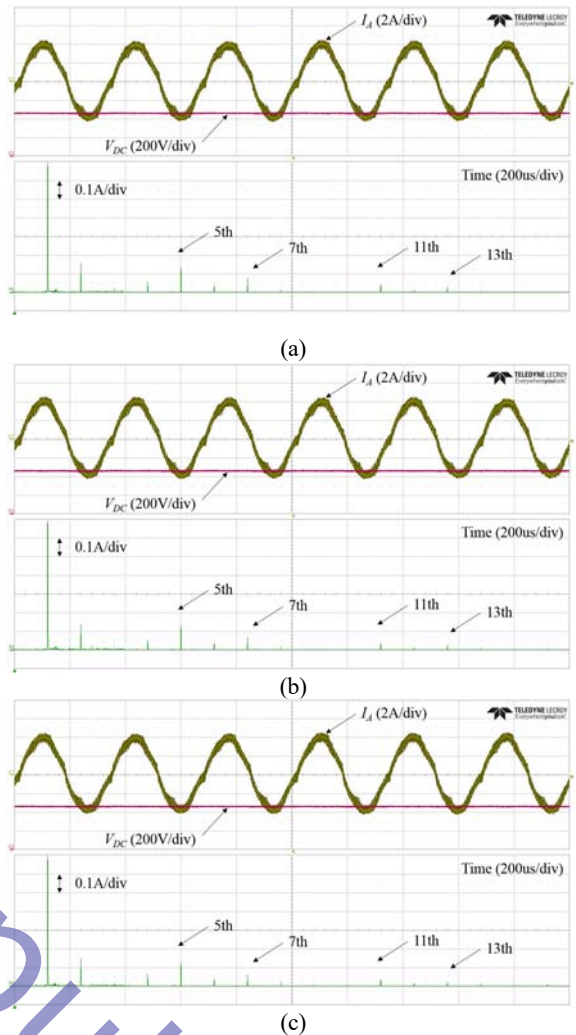

Fig. 22. Experiment results in 1 kW load condition. (a) Conventional CB-PWM. (b) Proposed synchronous CB-PWM. (c) Proposed synchronous CB-PWM and optimal reactive current injection.

controls the DC-link voltage to 450 V. The performance of the conventional CB-PWM is presented in Fig. 21(a). Distortion of the input current occurs at the zero-crossing point, and lower order harmonics such as the 5th, 7th, 11th, and 13th appear, as shown in the fast Fourier transform in Fig. 21(a). These results are similar to those in the simulations. THDi is approximately 6.6%.

The results of experiments conducted with the proposed CB-PWM technique are shown in Fig. 21(b). When the proposed synchronous CB-PWM switching method is applied, unnecessary voltage vectors are injected in the region in which the direction of the current and voltage of the rectifier is different. These voltage vectors increase the distortion of the input current at the zero-crossing point. The magnitudes of the 5th, 7th, 11th, and 13th harmonics, as shown in Fig. 21(b), are larger than those in Fig. 21(a). Therefore, THDi increases to 12.8% compared with the results depicted in Fig. 21(a).

The performance of the current injection technique with synchronous CB-PWM is shown in Fig. 21(c). The magnitudes of the 5th, 7th, 11th, and 13th harmonics are reduced and current distortion around the zero-crossing point is improved compared with the results shown in Figs. 21(a) and 21(b). THDi is approximately 1.1%, which is a 5% improvement compared to Fig. 21(a). We inject an optimal reactive current of 2.5 A to improve current quality. Given that the magnitude of the reactive current is extremely small compared with the active current (20 A), the Vienna rectifier can control the power factor to almost unity. Hence, the power factor is measured as 0.991 by the power analyzer, which is extremely close to a unity power factor.

The results of experiments conducted at 1 kW load condition are shown in Fig. 22. Other experimental conditions are the same as those used to obtain the results in Fig. 21. The distortion of the current at the zero-crossing point is similar with that in Figs. 22(a), (b), and (c), unlike the

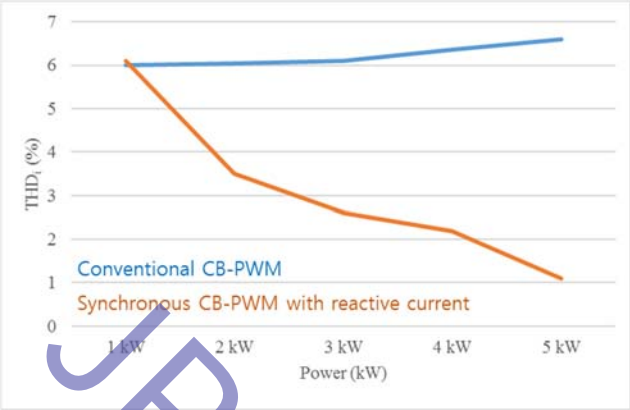

Fig. 23. Variation of THDi based on switching methods.

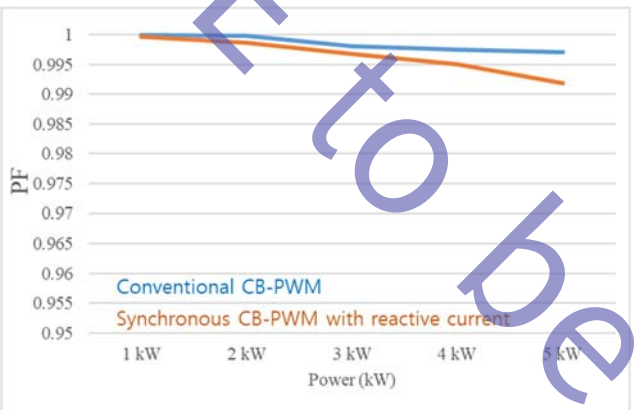

Fig. 24. Variation of power factor based on switching methods.

results in Fig. 21. In light load conditions, θ_Z is extremely small, such that the region in which the unnecessary voltage vectors are injected is narrow. Therefore, the current distortion at the zero-crossing point is not severe. In Fig. 22(a), θ_Z is approximately 1.3°. To compensate for θ_Z, 0.1 A reactive current is injected [Fig. 22(c)]. When comparing the THDi of Figs. 22(a) and (c), the results are similar by approximately 6%.

Experiments between 1 and 5 kW were also conducted to verify the proposed control method with the entire load. Current distortion depends on the magnitude of the input current, as described by (3). The magnitude of THDi based on the variation of the load is illustrated in Fig. 23. In the light load condition, current distortion is not severe regardless of the switching method because the impedance angle is extremely small, as dictated by (3). Therefore, the THDi of both switching methods are similar. As the load increases, the THDi of the conventional CB-PWM also increases because of the larger impedance angle. When the proposed synchronous CB-PWM algorithm is used, THDi decreases as the load increases because, as shown in Fig. 21(c), the magnitudes of the lower order harmonics are reduced by injecting the optimal reactive current. Therefore, the quality

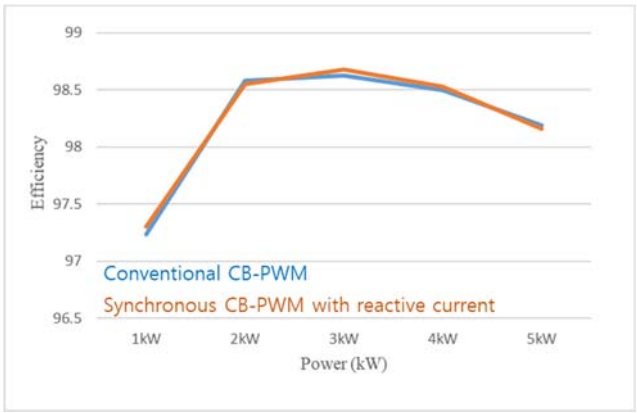

Fig. 25. Efficiency according to switching methods.

of the input current improves compared with that of the conventional CB- PWM.

The power factor based on the variation of the load is illustrated in Fig. 24. The optimal reactive currents are 0.10, 0.40, 0.91, 1.61, and 2.53 A per additional 1 kW load. The optimal reactive current is injected as the load current varies. The magnitude of the reactive current is small compared with the active current of the entire load. θ_Z increases with the load, as shown in (3). The magnitude of the optimal reactive current also increases, thereby improving the current distortion, and it is determined by (10). The power factor decreases as θ_Z increases, as shown in (12). Therefore, the power factor of the high power condition is lower than that of the light power condition. The results show that the power factor decreases as the load increases (Fig. 24). However, the power factor is above 0.99 for all considered loads. Consequently, the Vienna rectifier can control the power factor to almost unity.

The efficiency based on the switching methods is shown in Fig. 25. In the conventional CB-PWM, one of the back-to-back switches is triggered and the other is clamped to the ON state during a half period of the grid voltage. By contrast, in the proposed method, the back-to-back switches are operated synchronously. The switching number of the proposed method is twice as large as that of the conventional CB-PWM during a period of the grid voltage. However, in the almost region, the current path is the same as that in Fig. 7 regardless of the switching methods. When using the proposed switching method, in a switch in which current flows through anti-parallel diode, switching loss does not occur. Therefore, the mechanism of the power loss is the same as that for both switching methods. The experimental results indicate that the efficiency of both switching methods is similar for the entire load.

VI. Conclusions

We proposed a synchronous CB-PWM switching method for the Vienna rectifier with an algorithm to improve current

distortion. The Vienna rectifier typically requires six modulation signals if the conventional CB-PWM method is used. With the proposed synchronous CB-PWM method, the number of modulation signals is reduced to three from six. Therefore, reducing the cost and volume of the system is possible by using simplified gate driver circuits. However, when this method is applied, unnecessary voltage vectors are generated because of DCM, and currents are distorted around the zero-crossing point. A representative THDi of 6.6% was observed with the conventional CB-PWM switching method; this value increased to 12.8% with the proposed CB-PWM switching method at the rated power condition. Here, we proposed an optimal reactive current injection technique to improve current distortion. The optimal reactive current can be obtained simply based on the system parameters using the power factor angle and impedance angle. When this technique was used, the THDi was improved to 1.2%. Thus, the power factor can be controlled to above 0.99 because the magnitude of the injected reactive current is extremely small compared with the active current. The effectiveness of the proposed synchronous CB-PWM method with the reactive current injection algorithm was verified via PSIM simulation and experiments.

ACKNOWLEDGMENT

This work was supported by the Korea Institute of Energy Technology Evaluation and Planning (KETEP) and the Ministry of Trade, Industry & Energy (MOTIE) of the Republic of Korea (No. 20171210201100 and No. 20174030201660).

REFERENCES

[1] J. S. Park, M. J. Kim, H. S. Jeong, J. H. Kim, and S. W. Choi, "Development of 50kW high efficiency modular fast charger with wide charging voltage range," *Trans. Korean Inst. Power Electron*., Vol. 21, No. 3, pp. 267-274, Jun. 2016.

[2] A. Ansari, P, Cheng, and H.-J. Kim, "A 3 kW bidirectional DC-DC converter for electric vehicles," *J. Electr. Eng. Technol.*, Vol. 11, No. 4, pp. 860-868, Jul. 2016.

[3] S. G. Farkoush, C.-H. Kim, H.-C. Jung, S. Lee, N. T. Umpon, and S.-B. Rhee, "Power factor improvement of distribution system with EV chargers based on SMC method for SVC," *J. Electr. Eng. Technol*., Vol. 12, No. 4, pp. 860-868, Jul. 2017.

[4] S. Yang, J.-H, Park, and K.-B. Lee, "Current quality improvement for a Vienna rectifier with high-switching frequency," *Trans. Korean Inst. Power Electron*., Vol. 22, No. 2, pp. 181-184, Apr. 2017.

[5] A. K. Yadav, P. Gaur, S. K. Jha, J. R. P. Gupta, and A. P. Mittal, "Optimal speed control of hybrid electric vehicles," *J. Power Electron.*, Vol. 11, No. 4, pp. 393-400, Jul. 2011.

[6] A. Ghaderi, T. Umeno, Y. Amano, and S. Masaru, "A novel seamless direct torque control for electric drive vehicles," *J. Power Electron.*, Vol. 11, No. 4, pp. 449-455, Jul. 2011.

[7] N. T. B. Soeiro and J. W. Kolar, "Analysis of high-efficiency three-phase two- and three-level unidirectional hybrid rectifiers," *IEEE Trans. Ind. Electron*., Vol. 60, No. 9, pp. 3589-3601, Sep. 2013.

[8] M. S. Ortmann, S. A. Mussa, and M. L. Heldwein, "Three-phase multilevel PFC rectifier based on multistate switching cells," *IEEE Trans. Power Electron*., Vol. 30, No. 4, pp. 1843-1854, Apr. 2015.

[9] T. Friedli, M. Hartmann, and J. W. Kolar, "The essence of three-phase PFC rectifier systems – Part II," *IEEE Trans. Power Electron.*, Vol. 29, No. 2, pp. 543-560, Feb. 2014.

[10] A. Rajaei, M. Mohamadian, and A. Y. Varjani, "Vienna-rectifier-based direct torque control of PMSG for wind energy application," *IEEE Trans. Ind. Electron*., Vol. 60, No. 7, pp. 2919-2929, Jul. 2013.

[11] H. Chen and D. C. Aliprantis, "Analysis of squirrel-cage induction generator with VIENNA rectifier for wind energy conversion system," *IEEE Trans. Energy Convers*., Vol. 26, No. 3, pp. 967-975, Sep. 2011.

[12] J.-S. Lee, E. S. Lee, and K.-B. Lee, "Hybrid parallel three-level converter topology for large wind turbine generation systems," in *Proc, ISIE*, pp. 515–520, 2014.

[13] B. Kedjar, H. Y. Kanaan, and K. A. Haddad, "Vienna rectifier with power quality added function," *IEEE Trans. Ind. Electron*., Vol. 61, No. 8, pp. 3847-3856, Aug. 2014.

[14] J. Adhikari, P. IV, and S. K. Panda, "Reduction of input current harmonic distortions and balancing of output voltages of the Vienna rectifier under supply voltage disturbances," *IEEE Trans. Power Electron*., Vol. 32, No. 7, pp. 5802-5812, Jul. 2017.

[15] L. Hang, H. Zhang, S. Liu, X. Xie, C. Zhao, and S. Liu, "A novel control strategy based on natural frame for Vienna-type rectifier under light unbalanced-grid conditions," *IEEE Trans. Ind. Electron*., Vol. 62, No. 3, pp. 1353-1362, Mar. 2015.

[16] J.-S. Lee and K.-B. Lee, "A novel carrier-based PWM method for vienna rectifier with a variable power factor," *IEEE Trans. Ind. Electron*., Vol. 63, No.1, pp. 3-12, Jan. 2016.

[17] A. Rajaei, M. Mohamadian, and A. Y. Varjani, "Vienna-rectifier-based direct torque control of PMSG for wind energy application," *IEEE Trans. Ind. Electron.*, Vol. 60, No. 7, pp. 2919-2929, Jul. 2013.

[18] M. Leibl, J. W. Kolar, and J. Deuringer, "Sinusoidal input current discontinuous conduction mode control of the Vienna rectifier," *IEEE Trans. Power Electron*., Vol. 32, No. 11, pp. 8800-8812, Nov. 2017.

[19] J.-S. Lee and K.-B. Lee, "Carrier-based discontinuous PWM method for vienna rectifiers," *IEEE Trans. Power Electron*., Vol. 30, No. 6, pp. 2896-2900, Jun. 2015.

[20] J.-S. Lee and K.-B. Lee, "Performance analysis of carrier-based discontinuous PWM method for Vienna rectifiers with neutral-point voltage balance," *IEEE Trans. Power Electron*., Vol. 31, No. 6, pp. 4075–4084, Jun. 2016.

[21] P. Ide, F. Schafmeister, N. Fröhleke and H. Grotstollen, "Enhanced control scheme for three-phase three-level rectifier at partial load," *IEEE Trans. Ind. Electron*., Vol. 52, No. 3, pp. 719-726, Jun. 2005.

[22] S. Yang, J.-H, Park, and K.-B. Lee, "A carrier-based PWM with synchronous switching technique for a Vienna rectifier," in *Proc. PECON*, pp. 728-733, 2016.

Jin-Hyuk Park received his B.S. degree in Electronic Engineering from Ajou University, Suwon, Korea in 2013. He is presently working toward his Ph.D. degree in Electronic Engineering at Ajou University. His current research interests include power conversion and grid-connected systems.

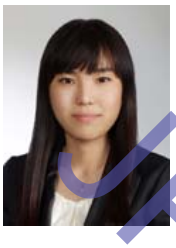

SongHee Yang received her B.S. and M.S degree in Electronic Engineering from Ajou University, Suwon, Korea in 2012 and 2017, respectively. Her current research interests include power conversion and grid-connected systems.

Kyo-Beum Lee received his B.S. and M.S. degrees in Electrical and Electronic Engineering from Ajou University, Suwon, Korea, in 1997 and 1999, respectively. He received his Ph.D. degree in Electrical Engineering from Korea University, Seoul, Korea, in 2003. From 2003 to 2006, he was with the Institute of Energy Technology, Aalborg University, Aalborg, Denmark. From 2006 to 2007, he was with the Division of Electronics and Information Engineering, Chonbuk National University, Jeonju, Korea. In 2007, he joined the School of Electrical and Computer Engineering, Ajou University. He is an Associate Editor of the IEEE Transactions on Power Electronics, the Journal of Power Electronics, and the Journal of Electrical Engineering and Technology. His current research interests include electric machine drives, renewable power generation, and electric vehicle applications.